Archival Report

Biological Psychiatry: GOS

MEF2C Hypofunction in GABAergic Cells Alters Sociability and Prefrontal Cortex Inhibitory Synaptic Transmission in a Sex-Dependent Manner

Jennifer Y. Cho, Jeffrey A. Rumschlag, Evgeny Tsvetkov, Divya S. Proper, Hainan Lang, Stefano Berto, Ahlem Assali, and Christopher W. Cowan

ABSTRACT

BACKGROUND: Heterozygous mutations or deletions of *MEF2C* cause a neurodevelopmental disorder termed MEF2C haploinsufficiency syndrome (MCHS), characterized by autism spectrum disorder and neurological symptoms. In mice, global *Mef2c* heterozygosity has produced multiple MCHS-like phenotypes. MEF2C is highly expressed in multiple cell types of the developing brain, including GABAergic (gamma-aminobutyric acidergic) inhibitory neurons, but the influence of MEF2C hypofunction in GABAergic neurons on MCHS-like phenotypes remains unclear.

METHODS: We employed GABAergic cell type–specific manipulations to study mouse *Mef2c* heterozygosity in a battery of MCHS-like behaviors. We also performed electroencephalography, single-cell transcriptomics, and patch-clamp electrophysiology and optogenetics to assess the impact of *Mef2c* haploinsufficiency on gene expression and prefrontal cortex microcircuits.

RESULTS: *Mef2c* heterozygosity in developing GABAergic cells produced female-specific deficits in social preference and altered approach-avoidance behavior. In female, but not male, mice, we observed that *Mef2c* heterozygosity in developing GABAergic cells produced 1) differentially expressed genes in multiple cell types, including parvalbumin-expressing GABAergic neurons, 2) baseline and social-related frontocortical network activity alterations, and 3) reductions in parvalbumin cell intrinsic excitability and inhibitory synaptic transmission onto deep-layer pyramidal neurons.

CONCLUSIONS: MEF2C hypofunction in female, but not male, developing GABAergic cells is important for typical sociability and approach-avoidance behaviors and normal parvalbumin inhibitory neuron function in the prefrontal cortex of mice. While there is no apparent sex bias in autism spectrum disorder symptoms of MCHS, our findings suggest that GABAergic cell-specific dysfunction in females with MCHS may contribute disproportionately to sociability symptoms.

https://doi.org/10.1016/j.bpsgos.2024.100289

The MEF2 (myocyte enhancer factor 2) family of transcription factors (MEF2A-D) regulates programs of gene expression that influence the proper development of the nervous, muscular, and immune systems and their adaptive responses throughout adulthood (1–13). *MEF2C* has emerged as a particularly important gene for brain development and function (7,14–16). Genome-wide association studies have linked *MEF2C* variants to increased risk for neuropsychiatric disorders, including schizophrenia, major mood disorders, and attention-deficit/hyperactivity disorder (17–22). De novo deletions or loss-of-function mutations in 1 gene copy cause MEF2C haploinsufficiency syndrome (MCHS), which is a neurodevelopmental disorder characterized by frequently observed symptoms of autism spectrum disorder (ASD), intellectual disability, absent or limited speech, seizures, and various motor and sensory abnormalities (23–34). The important function of MEF2C is conserved across species, as mice that lack 1 functional *Mef2c* allele ($Mef2c^{+/-}$) display numerous behavioral and brain circuit abnormalities that are reminiscent of MCHS (12–14,16).

In the developing mouse cortex and hippocampus, MEF2C is highly expressed in excitatory and inhibitory neurons and in microglia (7,9,16,35). Conditional *Mef2c* heterozygosity in most forebrain excitatory neurons (Emx1-lineage) has been shown to produce a subset of global $Mef2c^{+/-}$ mouse phenotypes, including hyperactivity and altered approach-avoidance behavior, but without influencing social preference (16), while conditional *Mef2c* heterozygosity in microglia (Cx3cr1-lineage) produce deficits in sociability and male-specific, enhanced jumping behavior (16). *Mef2c* heterozygosity using multiple Cre

ISSN: 2667-1743

driver lines and the corresponding behavioral phenotypes are outlined in Table 1.

GABAergic (gamma-aminobutyric acidergic) neurons make up ~10% to 30% of neurons within the cerebral cortex (36–40) and possess distinct morphological and electrophysiological properties that dictate their function (41). GABAergic interneurons, which are born in the ganglionic eminences and migrate into the developing cortex, are important for feedback and feedforward inhibition, forming a delicate balance of excitatory and inhibitory tone that is necessary for cortical information processing and neurotypical behavior (42–44). Perturbations to local cortical networks can cause hyper- or hypoexcitability (45), which can desynchronize neuronal oscillations that coordinate the activity of different brain regions to guide complex behavior (46). Abnormalities in GABAergic inhibitory synaptic transmission, particularly in the prefrontal cortex (PFC), have been linked to altered cognition and social behaviors (47). Shifts in the balance of excitatory and inhibitory medial PFC (mPFC) synaptic transmission have been implicated in ASD and other neuropsychiatric disorders (44). Previous studies have revealed that conditional knockout of both *Mef2c* alleles in GABAergic neuron precursors (Dlx5/6-lineage) disrupted differentiation of parvalbumin (PV)–positive GABAergic neurons (8), but the impact of *Mef2c* heterozygosity in PV cell precursors, or more broadly in GABAergic cells, remains unknown.

METHODS AND MATERIALS

Animals

Mice (*Mus musculus*) were group housed (2–5 animals per cage) with same-sex littermates in a reverse 12-hour light/dark cycle facility with ad libitum access to food and water. We generated cell type–specific *Mef2c* conditional heterozygous (cHet) mice by crossing $Mef2c^{fl/+}$ mice (RRID:MGI:3719006) with Vgat-Cre (Jackson Laboratory, #028862), Sst-Cre (Jackson Laboratory, #013044), or Vip-Cre (Jackson Laboratory, #010908) mice. Experimenters were blinded to mouse genotype during experimentation, data collection, and analysis. Animals were tested under guidelines provided by the Medical University of South Carolina Institutional Animal Care and Use Committee and the National Institutes of Health.

RESULTS

Mouse Model of *Mef2c* Conditional Heterozygosity in GABAergic Inhibitory Populations

To study the impact of MEF2C hypofunction in GABAergic cell populations during development, we bred Vgat-Cre mice, which express Cre recombinase broadly in early developing GABAergic neurons (48), with floxed *Mef2c* loss-of-function mice (49) to create offspring that are GABAergic cell-specific *Mef2c* heterozygous mutants ($Mef2c^{fl/+}$;Vgat-Cre or *Mef2c* $cHet^{Vgat}$). Vgat-Cre crossed with Ai14 reporter mice produced the expected pattern of recombination in GABAergic populations as validated in our laboratory (48,50) (Figure S1A in Supplement 1). Previous studies in our laboratory have confirmed that Vgat-cre and Ai14 recombination occurs on or before embryonic day E15.5 (50). Conditional knockout of both *Mef2c* alleles in GABAergic cells (*Mef2c* cKO^{Vgat}) resulted in postnatal lethality (i.e., around postnatal days 15 to 25) in most of the mutant mice (~70–90%; J Cho, B.S., 2020–2022). One *Mef2c* cKO^{Vgat} male that escaped postnatal lethality displayed severe motor impairments (J Cho, B.S., July 2020). In contrast, loss of only 1 *Mef2c* allele in GABAergic cells (*Mef2c* $cHet^{Vgat}$) resulted in the expected Mendelian frequency and life spans (Figure S1B in Supplement 1).

Next, we subjected the 8- to 12-week-old *Mef2c* $cHet^{Vgat}$ and littermate control male and female mice to a battery of behavior tests (Figure 1). Analysis of maternal separation–induced ultrasonic vocalizations (USVs) at postnatal days 4, 7, and 10 revealed no difference in the number of USVs produced (Figure S1C in Supplement 1). As young adults, *Mef2c* $cHet^{Vgat}$ mice displayed normal locomotion and jumping in a novel environment (Figure 1B, C). In the Y-maze, *Mef2c* $cHet^{Vgat}$ mice displayed fewer correct spontaneous alternations (Figure 1D; Figure S1D in Supplement 1), suggesting a deficit in spatial working memory. In the elevated plus maze (EPM), female, but not male, *Mef2c* $cHet^{Vgat}$ mice spent significantly more time in the unprotected, open arms of the EPM (Figure 1E), revealing a female-specific change in neurotypical approach-avoidance behavior. In the 3-chamber social interaction test, only female *Mef2c* $cHet^{Vgat}$ mice showed a significant deficit in social preference for a novel, sex-matched mouse compared with a novel object (Figure 1F; Figure S1E in Supplement 1). Finally, *Mef2c* $cHet^{Vgat}$ mice displayed typical freezing behaviors in the context and cued Pavlovian fear conditioning tests, similar to the global $Mef2c^{+/-}$ mice (16) (Figure 1; Figure S1F in Supplement 1).

Mef2c Heterozygosity Within Individual Major GABAergic Interneuron Subpopulations Alone Does Not Reproduce *Mef2c* $cHet^{Vgat}$ Mouse Behavioral Phenotypes

Next, we examined whether behavioral phenotypes in *Mef2c* $cHet^{Vgat}$ mice might be produced primarily by major GABAergic interneuron subclasses, namely the somatostatin (SST), vasoactive intestinal peptide (VIP), and PV-expressing populations. However, neither the *Mef2c* $cHet^{Sst}$ ($Mef2c^{fl/+}$;Sst-Cre or *Mef2c* $cHet^{Sst}$) nor the *Mef2c* $cHet^{Vip}$ ($Mef2c^{fl/+}$;Vip-Cre or *Mef2c* $cHet^{Vip}$) mice displayed notable behavioral differences from littermate controls in the battery of assessed behaviors (Figure 2A–H; Figure S2A–J in Supplement 1). Female *Mef2c* $cHet^{Sst}$ mice displayed an increase in freezing time during fear conditioning training compared with control female mice, suggesting a heightened response to tone-shock pairings (Figure S2C in Supplement 1). Additionally, male *Mef2c* $cHet^{Vip}$ mice exhibited a significant increase in jump counts, which suggests a possible role for MEF2C in VIP-expressing inhibitory neurons to regulate repetitive behaviors (Figure S2G in Supplement 1); however, this was not observed in the pan-GABAergic context (Figure 1C). We previously reported that *Mef2c* $cHet^{Pv}$ mice did not display the behavioral phenotypes observed in *Mef2c* $cHet^{Vgat}$ mice (16). However, because Pv-Cre expression begins at postnatal day 8 or later (16,51), we cannot preclude the possibility that *Mef2c* heterozygosity in developmental precursors of PV neurons before the second postnatal week of life influences the expression of abnormal phenotypes. Taken together, these findings indicate that *Mef2c* heterozygosity in embryonic SST or VIP cells or in

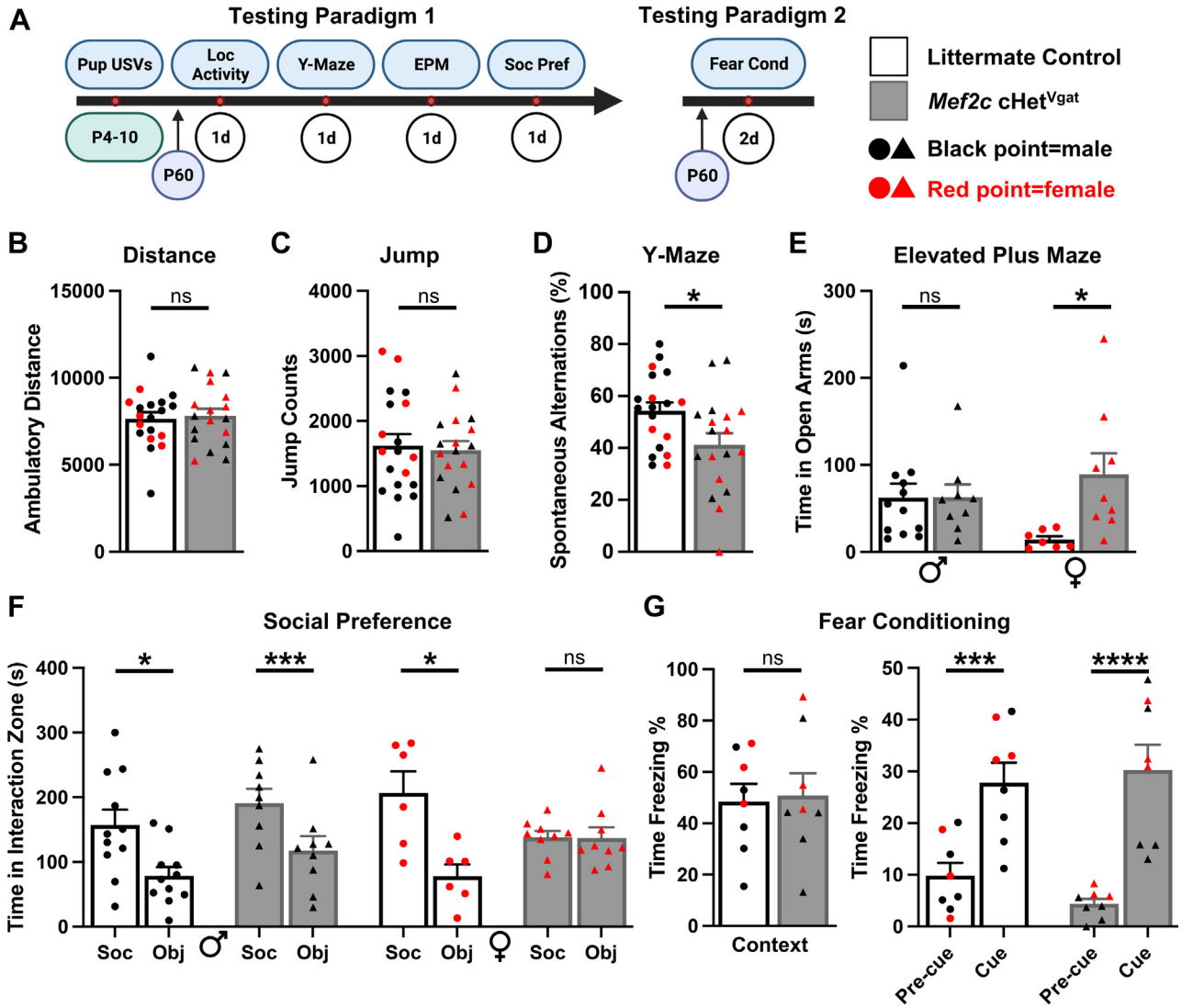

Figure 1. *Mef2c* cHet^{Vgat} mice display spatial working memory deficits, altered approach avoidance, and reduced social preference. **(A)** Behavior battery paradigms and legend. **(B, C)** *Mef2c* cHet^{Vgat} mice exhibited normal locomotor activity as assessed by distance traveled and jump counts in a 1-hour locomotor assay. **(D)** *Mef2c* cHet^{Vgat} mice performed worse on the Y-maze, a spatial working memory assay, with significantly fewer correct spontaneous alternations than control mice. **(E)** Female, but not male, *Mef2c* cHet^{Vgat} mice displayed altered approach-avoidance behaviors on the EPM. **(F)** Unlike control mice, female *Mef2c* cHet^{Vgat} mice showed no preference for the social target over the novel object. Female control, male control, and male *Mef2c* cHet^{Vgat} mice showed a statistically significant social preference. **(G)** *Mef2c* cHet^{Vgat} and control mice displayed normal freezing in the context (left) and cue (right) fear conditioning tests. Red data points represent females, circles represent control animals, and triangles represent *Mef2c* cHet^{Vgat} mice. Data are reported as mean ± SEM. Statistical significance was determined by unpaired *t* test for **(B)**, **(C)**, **(D)**, and **(G)** (left). Statistical significance was determined by analysis of variance for **(E)** (2-way), **(F)** (3-way), and **(G)** (right) (2-way). ns = not significant ($p > .05$), *$p < .05$, ***$p < .005$, ****$p < .001$. For **(B–E)**, there were 19 mice (12 male, 7 female) in the control group and 18 mice (9 male, 9 female) in the *Mef2c* cHet^{Vgat} group. For **(F)**, there were 17 mice (11 male, 6 female) in the control group and 18 mice (9 male, 9 female) in the *Mef2c* cHet^{Vgat} group. For **(G)**, there were 8 mice (5 male, 3 female) in the control group and 8 mice (5 male, 3 female) in the *Mef2c* cHet^{Vgat} group. Outliers were removed using the Grubbs' test. Control mice include Cre-negative and Cre-positive mice. cHet, conditional heterozygous; Cond, conditioning; EPM, elevated plus maze; Loc, locomotor; Obj, object interaction zone; Soc, social interaction zone; Soc Pref, 3-chamber social interaction assay; USV, ultrasonic vocalization.

postnatal PV cells does not, at least by itself, account for *Mef2c* cHet^{Vgat} behavior phenotypes.

Mef2c cHet^{Vgat} Mice Display Female-Specific Frontocortical Gamma Power Alterations

To detect differences in cortical processing of social information, we recorded in vivo brain activity using electroencephalography (EEG). *Mef2c* cHet^{Vgat} and control mice were tethered and acclimated for 10 minutes in the novel open field arena. Mice were then introduced to a novel age- and sex-matched mouse for 10 minutes (Figure 3A). Relative EEG power in the PFC was measured during active social interaction and noninteraction periods throughout the social encounter (Figure 3B). Gamma power

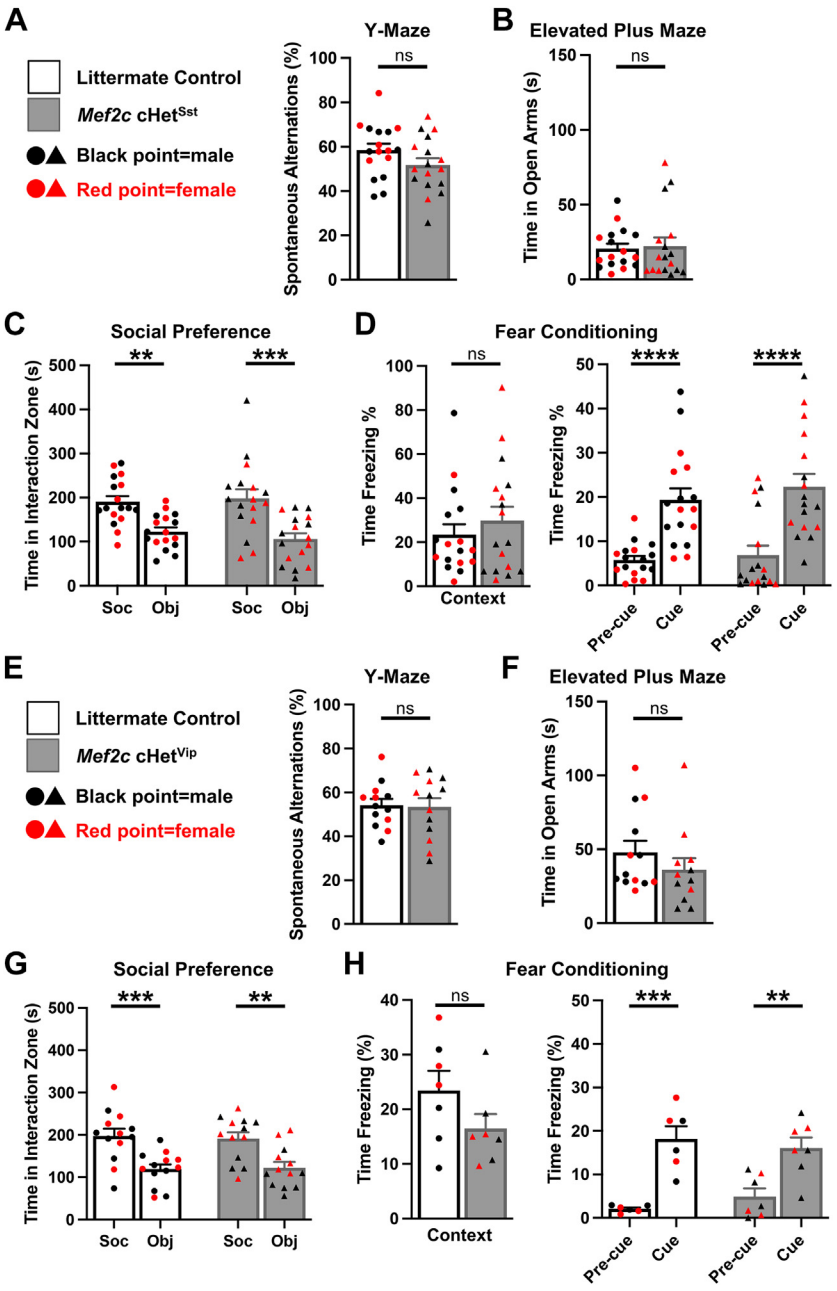

Figure 2. Conditional *Mef2c* heterozygosity in SST or VIP neurons alone does not recapitulate MEF2C haploinsufficiency syndrome–relevant *Mef2c* cHet^{Vgat} behavioral phenotypes. **(A)** Control and *Mef2c* cHet^{Sst} mice performed similarly on the Y-maze, with no significant difference in percentage of correct spontaneous alternations. **(B)** *Mef2c* cHet^{Sst} mice exhibited normal approach-avoidance behaviors on the elevated plus maze and spent similar amounts of time in the open arms. **(C)** Control and *Mef2c* cHet^{Sst} mice displayed a strong social preference for the social target over the novel object. **(D)** *Mef2c* cHet^{Sst} mice froze similarly in the context and cue tests in fear conditioning. **(E)** *Mef2c* cHet^{Vip} mice displayed normal spatial working memory on the Y-maze compared with littermate control mice. **(F)** *Mef2c* cHet^{Vip} mice displayed normal approach-avoidance behaviors on the elevated plus maze. **(G)** *Mef2c* cHet^{Vip} and control mice strongly preferred the social target over the novel object. **(H)** *Mef2c* cHet^{Vip} mice had normal freezing in the context (left) and cue (right) fear conditioning tests. Red data points represent females, circles represent control animals, and triangles represent *Mef2c* cHet mice. Data are reported as mean ± SEM. Statistical significance was determined by unpaired *t* test for **(A)**, **(B)**, **(D)** (left), **(E)**, **(F)**, and **(H)** (left). Statistical significance was determined by analysis of variance for **(C)** (2-way), **(D)** (right) (2-way), **(G)** (2-way), and **(H)** (right) (2-way). ns = not significant ($p > .05$), $^{**}p < .01$, $^{***}p < .005$, $^{****}p < .001$. For **(A–D)**, there were 17 mice (9 male, 8 female) in the control group and 17 mice (9 male, 8 female) in the *Mef2c* cHet^{Sst} group. For **(E, G)**, there were 13 mice (7 male, 6 female) in the control group and 13 mice (7 male, 6 female) in the *Mef2c* cHet^{Vip} group. For **(F)**, there were 13 mice (7 male, 6 female) in the control group and 12 mice (6 male, 6 female) in the *Mef2c* cHet^{Vip} group. For **(H)**, there were 7 mice (4 male, 3 female) in the control group and 7 mice (4 male, 3 female) in the *Mef2c* cHet^{Vip} group. Outliers were removed using the Grubbs' test. Control mice as a group include Cre-positive mice. cHet, conditional heterozygous; Obj, object interaction zone; Soc, social interaction zone; SST, somatostatin; VIP, vasoactive intestinal peptide.

was found to be significantly higher during periods of social interaction than noninteraction for all groups except for control males (Figure 3C–E), and females had significantly higher gamma power than males (Figure 3E). We found no significant difference between male and female control mice in low gamma power during noninteraction periods; conversely, during periods of social interaction, we detected a significant decrease in low gamma power in males, perhaps due to varying arousal states, estrus status, and differing social dynamics (Figure 3E). During social interaction, there was higher gamma power in control females than *Mef2c* cHet^{Vgat} females, while no differences were detected in the male *Mef2c* cHet^{Vgat} and control male mice (Figure 3E). These findings demonstrate baseline gamma power differences between control mice in response to social information and increased gamma power during social interaction in control females compared with female *Mef2c* cHet^{Vgat} mice.

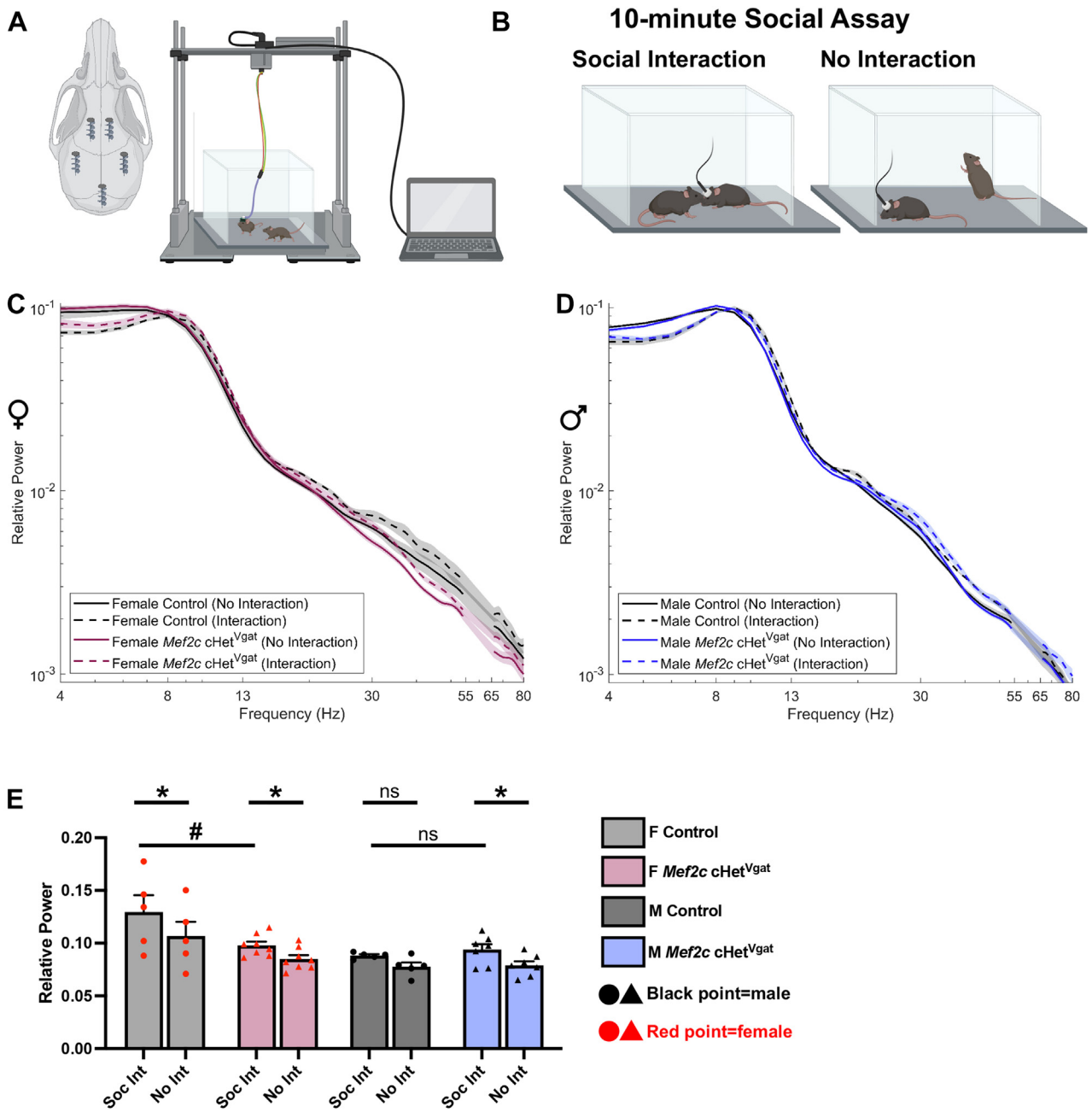

Figure 3. Female *Mef2c* cHet^{Vgat} mice display reduced medial prefrontal cortex gamma power during social behavior. **(A)** Screws were placed epidurally atop the prefrontal cortex, somatosensory cortex, and cerebellum. The experimental mouse was placed in an open arena and tethered to a custom electroencephalography recording system. **(B)** Social interaction in video recordings were detected using BORIS. Social bouts were characterized as mutual orientation (snout to snout), proximity, and physical interaction with the other animal (snout to body). **(C, D)** Visual representation of the relative power at low gamma frequencies during social interaction and during noninteraction throughout the 10-minute social exploration period. **(E)** Quantification of relative power during periods of social interaction and periods of noninteraction. According to the post hoc test of marginal mean difference (*emmeans* package, R language), gamma power was higher during social interaction compared with noninteraction (estimated mean difference = 0.015, SE = 0.002, t_{21} = 8.993, $p < .0001$). Females had higher gamma power compared with males (estimated mean difference = 0.020, SE = 0.020, t_{21} = 2.955, p = .008). Post hoc pairwise comparisons using the Tukey method to correct for multiple comparisons showed higher gamma power in control females than in *Mef2c* cHet^{Vgat} females (estimated mean difference = 0.032, SE = 0.010, t_{24} = 3.249, adjusted p = .058), whereas control males did not have significantly different gamma power compared with *Mef2c* cHet^{Vgat} males (estimated mean difference = −0.006, SE = 0.010, t_{24} = −0.558, adjusted p = .999). For **(C–E)**, there were 10 mice (5 male, 5 female) in the control group and 15 mice (7 male, 8 female) in the *Mef2c* cHet^{Vgat} group; each data point represents an average of 2 prefrontal cortex recordings (1 in each hemisphere). #$p < .1$, *$p < .05$. Control mice include Cre-negative and Cre-positive mice. cHet, conditional heterozygous; F, female; M, male; no int, no interaction; ns, not significant; Soc int, social interaction.

Single-Cell Transcriptomic Analysis of *Mef2c* cHet^{Vgat} Mice Reveals Significant Dysregulation of Gene Expression in Multiple GABAergic Cell Types of the PFC

While MEF2C is expressed in GABAergic neurons throughout the brain, and the complex behaviors we analyzed in this study involve distributed neural circuits functioning across multiple brain regions, we chose to focus on PFC transcriptomics because social interaction, approach-avoidance, and working memory are all dependent on the mPFC (44,52–54). Accordingly, we examined the impact of GABAergic cell type–specific *Mef2c* heterozygosity on cell type distribution and gene expression in this central brain region. Toward this end, we isolated and pooled mPFC tissue from 3 female *Mef2c* cHet^{Vgat} and 3 female control mice and performed single-nucleus RNA sequencing (snRNA-seq) (Figure 4A; Figure S3A–E in Supplement 1). After quality-control filtering, we retained a total of 23,599 nuclei for snRNA-seq (Figure S3A–C in Supplement 1). We applied uniform manifold approximation and projection dimensionality reduction and Leiden clustering to transcriptomic datasets and identified 22 distinct cell-type clusters (Figure 4B). We profiled all major mPFC cell types of the brain—excitatory neurons, inhibitory neurons, astrocytes, microglia, oligodendrocytes, oligodendrocyte progenitor cells, vascular cells, and endothelial cells. Clusters were annotated based on known marker genes (Figure 4C). Next, we examined the composition of each cluster in the context of *Mef2c* cHet^{Vgat} mice and found no significant differences in overrepresented or underrepresented cell types (Figure S3C in Supplement 1). As expected, *Mef2c* messenger RNA was enriched predominantly in excitatory and inhibitory neurons and microglia, and the relative proportions of the various mPFC cell populations were similar in control and *Mef2c* cHet^{Vgat} mice (Figure 4D).

To gain more insight into the effect of *Mef2c* at a cell-type level, we performed differential gene expression analysis (Table S1 in Supplement 2; Table S2 in Supplement 3). We found numerous differentially expressed genes (DEGs) in female *Mef2c* cHet^{Vgat} mice. As expected, a large proportion of DEGs in *Mef2c* cHet^{Vgat} mPFC was observed in GABAergic interneuron clusters (Figure 4E). Nonetheless, we observed DEGs in excitatory glutamatergic neurons, microglia, oligodendrocytes, and vascular cell clusters, presumably from cell nonautonomous influences of *Mef2c* heterozygosity in GABAergic cells. Within the GABAergic cell clusters, the largest number of DEGs was observed in the Lamp5$^+$ (lysosome-associated membrane protein 5) and Pvalb$^+$ inhibitory cell types, with fewer DEGs in the Sst$^+$ and Vip$^+$ inhibitory neuron clusters (Figure 4E). Moreover, we found that DEGs were highly specific, with minimal overlap between inhibitory cell types (Figure 4F). Because *MEF2C* is a high-risk neurodevelopmental disorder gene, we advanced our understanding of ASD risk by performing gene-set enrichment with known ASD genes. Interestingly, among the inhibitory cell types, we found a significant enrichment (false discovery rate $<$ 0.05) in the Inh_Pvalb$^+$ cluster for high-confidence autism-linked genes (Figure 4), such as *Grin2a*, *Nrg1*, *Grik2*, and *Reln* (Figure 4G, H). Furthermore, we investigated the overlap between genes affected in the mPFC of *Mef2c* cHet^{Vgat} mice and snRNA-seq data from postmortem brains of humans with ASD. Interestingly, Inh_Pvalb DEGs were enriched for genes perturbed in human PVALB neurons, thus underscoring the key role of *Mef2c* in regulating ASD genes in PV inhibitory neurons (Figure S3D in Supplement 1). Next, we performed functional enrichment for inhibitory neuron DEGs and found high cell type-specificity. We found that in the Inh_Pvalb$^+$ cluster, DEGs showed significant enrichment of genes linked to axon development, synaptic transmission, synapse organization, synaptic signaling, and cell junction assembly (Figure 4I; Table S3 in Supplement 4). To further support the role of *Mef2c* in the regulation of inhibitory cell type DEGs, we analyzed MEF2C chromatin immunoprecipitation sequencing data from an independent study (55) and found significant enrichment in Inh_Pvalb$^+$ and Inh_Lamp5$^+$ DEGs for genes bound by MEF2C in multiple genomic regions (Figure S4E in Supplement 1).

To explore snRNA-seq data at a systems level, we specifically analyzed inhibitory neurons by using a weighted co-expression network method (Figure 4J). In total, we found 8 co-expression modules, 4 of which were significantly correlated with genotype, and their module eigengene showed significant differences between *Mef2c* cHet^{Vgat} and control mice (Figure 4K). Moreover, using differential module eigengene analysis, we found that M6 was the most differentially expressed between *Mef2c* cHet^{Vgat} and control mice (Figure 4L). Additionally, the M6 module showed enrichment for the *Mef2c* binding motif, and its overall expression is enriched in Inh_Pvalb$^+$ (Figure 4M–O). Finally, we highlighted the top 25 hub genes of M6 and detected *Mef2c*, as well as genes like *Cntnap4*, which contribute to GABAergic synaptic transmission (56,57). Thus, our differential expression analysis and system-level network analysis facilitated the identification of cell type–specific disease biology driven by *Mef2c* heterozygosity and highlighted a key role for MEF2C in regulating the transcriptional landscape of PV inhibitory neurons.

MEF2C Hypofunction in GABAergic Neurons Reduces PV Cell Intrinsic Excitability and Inhibitory Synaptic Transmission in the mPFC

While conditional embryonic knockout of *Mef2c* in Dlx5/6-Cre lineage GABAergic cells dramatically reduces PV cell differentiation (8), our snRNA-seq studies revealed no differences in the number of Inh_Pvalb$^+$ cells in female *Mef2c* cHet^{Vgat} mice compared with female control mice (Figure S3C in Supplement 1). We also detected no difference by genotype in *Pvalb* messenger RNA levels in the P56 mPFC (Figure 5A) and no difference in PV$^+$ neuron density in the mPFC of *Mef2c* cHet^{Vgat} mice (Figure 5B), suggesting that 1 functional *Mef2c* allele is sufficient for PV cell differentiation.

Because there were numerous *Mef2c* cHet^{Vgat} DEGs in the PV cell cluster linked to synaptic transmission (Figure 4I), we examined the intrinsic and synaptic properties of PV interneurons in *Mef2c* cHet^{Vgat} mice at P56. We performed whole-cell patch-clamp recordings of PV cells in current clamp mode and analyzed action potentials produced with current stimulation. While there was no apparent change in rheobase, PV cells from female (Figure 5C), but not male (Figure S4A in Supplement 1), *Mef2c* cHet^{Vgat} mice showed a significant reduction in action potentials elicited over a wide range of current steps, revealing a reduction in PV cell intrinsic excitability. In voltage-clamp mode, we did not observe any differences by genotype or sex on excitation/inhibition ratio

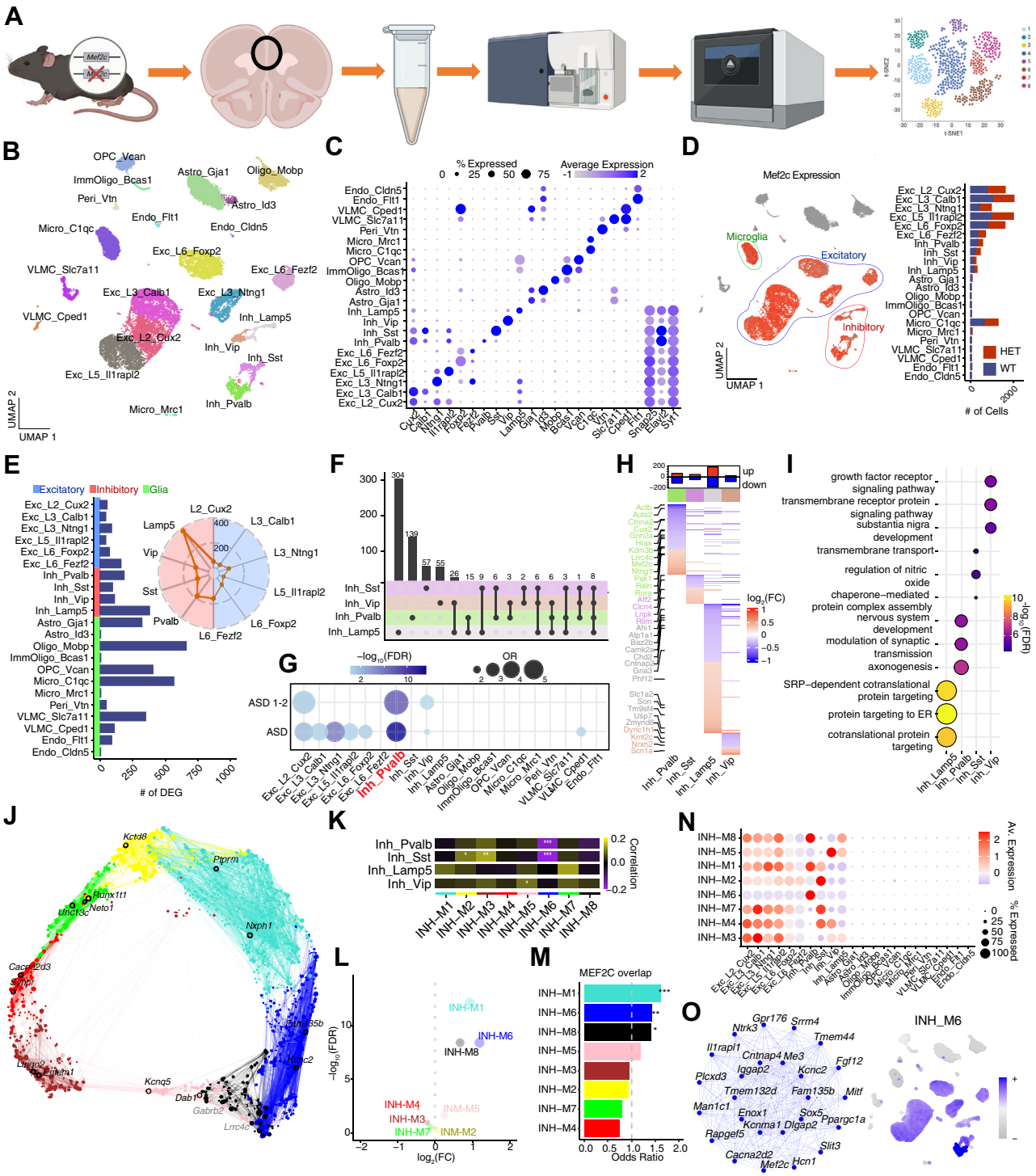

Figure 4. Single-nucleus RNA sequencing in female *Mef2c* cHet^{Vgat} mice. **(A)** Schematic representation of the mice, prefrontal cortex dissection, nuclear dissociation and isolation, fluorescence-activated nucleus sorting, sequencing, and downstream bioinformatic approaches used in this study. **(B)** UMAP visualization of the single-nuclei data. Dots correspond to individual nuclei for 23,599 nuclei profiled with single-nucleus RNA sequencing. **(C)** Dot plot depicting the expression of known neuronal and glia markers. Gradient color corresponds to the expression level, whereas dot size corresponds to the percentage of nuclei expressing the marker. **(D)** UMAP visualization depicting *Mef2c* expression distribution in the cell types identified. (Right) A stacked bar plot showing the proportion of nuclei within a cell type expressing *Mef2c* in *Mef2c* cHet^{Vgat} and control mice. **(E)** Bar plot depicting the number of genes differentially expressed in each cell type identified. (Right) Spider plot showing the number of DEGs in neuronal populations (red = inhibitory neurons, blue = excitatory neurons). **(F)** UpSet plot summarizing the overlap between DEGs in inhibitory neurons. **(G)** Bubble chart showing the enrichment of ASD genes in cell

calculated from evoked excitatory postsynaptic currents (AMPA-mediated currents) and evoked inhibitory postsynaptic currents (IPSCs) (GABA-mediated currents) onto PV cells (Figure S4B, C in Supplement 1), suggesting preserved synaptic transmission onto PV cells in *Mef2c* cHet^{Vgat} mice at P56. Moreover, similar spontaneous excitatory postsynaptic current frequency and amplitude onto PV cells supported typical levels of excitatory transmission onto PV cells in *Mef2c* cHet^{Vgat} mice (Figure S4D, E in Supplement 1). Next, to assess the output from PV cells onto deep-layer pyramidal neurons, we elicited optogenetically evoked IPSCs (oeIPSCs) onto deep-layer pyramidal neurons. We observed that female (Figure 5D), but not male (Figure S4F in Supplement 1), *Mef2c* cHet^{Vgat} mice displayed a decrease in oeIPSC amplitude onto pyramidal neurons. However, there was no effect by genotype on the oeIPSC paired-pulse ratio (PPR) (Figure S4G in Supplement 1), suggesting that the reduction in inhibitory synaptic transmission onto deep-layer pyramidal neurons is not caused by a change in PV cell presynaptic function. When we recorded spontaneous IPSCs (sIPSCs) of all GABAergic inputs onto the deep-layer pyramidal neurons, we observed a small but significant reduction in the frequency of sIPSCs in female (Figure 5E), but not male (Figure S4H in Supplement 1), *Mef2c* cHet^{Vgat} mice. No changes in sIPSC amplitude were observed in pyramidal cells (Figure 5E; Figure S4H in Supplement 1), and we detected no differences in GABAergic PPR in pyramidal cells (Figure S4I in Supplement 1). We did not observe any difference by sex or genotype on membrane resistance, membrane capacitance, or resting membrane potential in PV cells of control or *Mef2c* cHet^{Vgat} mice (Figure S4J–L in Supplement 1).

Taken together, these data suggest that *Mef2c* heterozygosity in GABAergic cells produces significant sex-specific reductions in PV interneuron excitability and inhibitory synaptic transmission onto deep-layer mPFC pyramidal neurons.

DISCUSSION

MCHS is characterized by numerous neurological symptoms (23–34), and a mouse model of MCHS (global *Mef2c*$^{+/-}$) has shown face-valid behavioral differences that are reminiscent of MCHS symptoms (14,16). MEF2C is highly expressed in multiple cell types, but whether MEF2C haploinsufficiency in certain cell types disproportionately contributes to MCHS-related phenotypes remains unclear. In this study, we examined *Mef2c's* role in GABAergic cell populations (Vgat-lineage) for MCHS-like behaviors. In *Mef2c* cHet^{Vgat} mice, we detected 2 behavioral differences that are seen in global *Mef2c*$^{+/-}$ mice: 1) decreased social preference and 2) reduced avoidance of the unprotected arms of the EPM. However, unlike global *Mef2c*$^{+/-}$ mice, relevant *Mef2c* cHet^{Vgat} behavior differences were only present in females. Analysis of EEGs in the frontal cortex of female, but not male, *Mef2c* cHet^{Vgat} mice revealed a reduction of EEG power in the gamma bands during social engagement, suggesting sex-specific alterations in fronto-cortical information processing. Analysis of cell types in the mPFC of female *Mef2c* cHet^{Vgat} and control mice exposed DEGs in several populations, including robust changes in PV^{+} neurons and strong evidence for *Mef2c*'s role as a hub gene in the PV cell population. Analysis of PV cells in the mPFC of *Mef2c* cHet^{Vgat} mice revealed a significant reduction in intrinsic excitability and inhibitory synaptic transmission onto mPFC deep-layer pyramidal neurons. Taken together, our findings uncover an interaction between *Mef2c* heterozygosity in GABAergic cells and sex for social preference and anxiety-like behaviors, and they demonstrate that MEF2C hypofunction in one or more GABAergic cell populations is sufficient to alter mPFC-linked neurotypical behaviors, gene expression, and inhibitory microcircuit function.

Notably, we did not directly assess whether *Mef2c* floxed mice or Cre-positive mice conferred biochemical or behavioral phenotypes in the current study; however, we have previously utilized *Mef2c* floxed mice as Cre-negative control mice, and we did not detect overt abnormal behavioral phenotypes (7,16). We cannot exclude the possibility that the *Mef2c* floxed allele or the presence of Cre recombinase perturbs natural behavior, thereby differentiating these mice from true wild-type mice. Moreover, a limitation of our model is that we are assessing the isolated role of MEF2C in inhibitory neurons and the following compensatory or cell nonautonomous changes, such as circuit function, that are unique to this manipulation. These findings do not fully translate to circuit changes present in *Mef2c* global heterozygous mice, which are found across many different cell types and relate more closely to MCHS.

In this study, we focused on the mPFC due to its strong connection to social behavior, ASD, and approach-avoidance behavior. Moreover, PV interneurons in the mPFC play important roles in social behavior (58,59). The PFC plays an essential role in social motivation (60), social information processing (61), behavioral flexibility, response inhibition, attention, and emotion (62). Functional magnetic resonance imaging studies of adults with ASD have reported weaker functional

type–specific DEGs. Gradient color corresponds to the $-\log_{10}$(FDR), whereas dot size corresponds to the OR (Fisher's exact test). **(H)** Heatmap visualizing the DEGs in inhibitory neurons ranked by fold change difference between *Mef2c* cHet^{Vgat} and control mice. Highlighted genes are associated with ASD. **(I)** Bubble chart highlighting the top 3 functional categories enriched in DEGs of inhibitory cell types. Gradient color and dot size correspond to the $-\log_{10}$(FDR). **(J)** Network visualization of the 8 inhibitory modules identified by co-expression analysis. **(K)** Heatmap showing the correlation between module eigengene and genotype. Stars correspond to statistically significant correlations. Gradient corresponds to positive or negative correlation. **(L)** Volcano plot depicting module eigengene differences between *Mef2c* cHet^{Vgat} and control mice. The x-axis shows the $\log_2$(FC), whereas the y-axis shows the $-\log_{10}$(FDR). Analysis was performed using a linear model. **(M)** Bar plot showing the enrichment of MEF2C motifs in the inhibitory-associated modules. Stars correspond to statistically significant enrichment. **(N)** Bubble chart depicting the overall expression of genes within the modules in each cell type. Gradient color corresponds to the expression level, whereas dot size corresponds to the percentage of nuclei expressing the genes within the modules. **(O)** Co-expression plot for INH-M6 showing the top 25 hub genes. (Right) UMAP showing the relative expression of INH-M6. Control mice as a group include Cre-positive mice. ASD, autism spectrum disorder; cHet, conditional heterozygous; DEG, differentially expressed gene; ER, endoplasmic reticulum; FC, fold change; FDR, false discovery rate; HET, heterozygous; OR, odds ratio; SRP, signal recognition particle; t-SNE, t-distributed stochastic neighbor embedding; UMAP, uniform manifold approximation and projection; WT, wild-type.

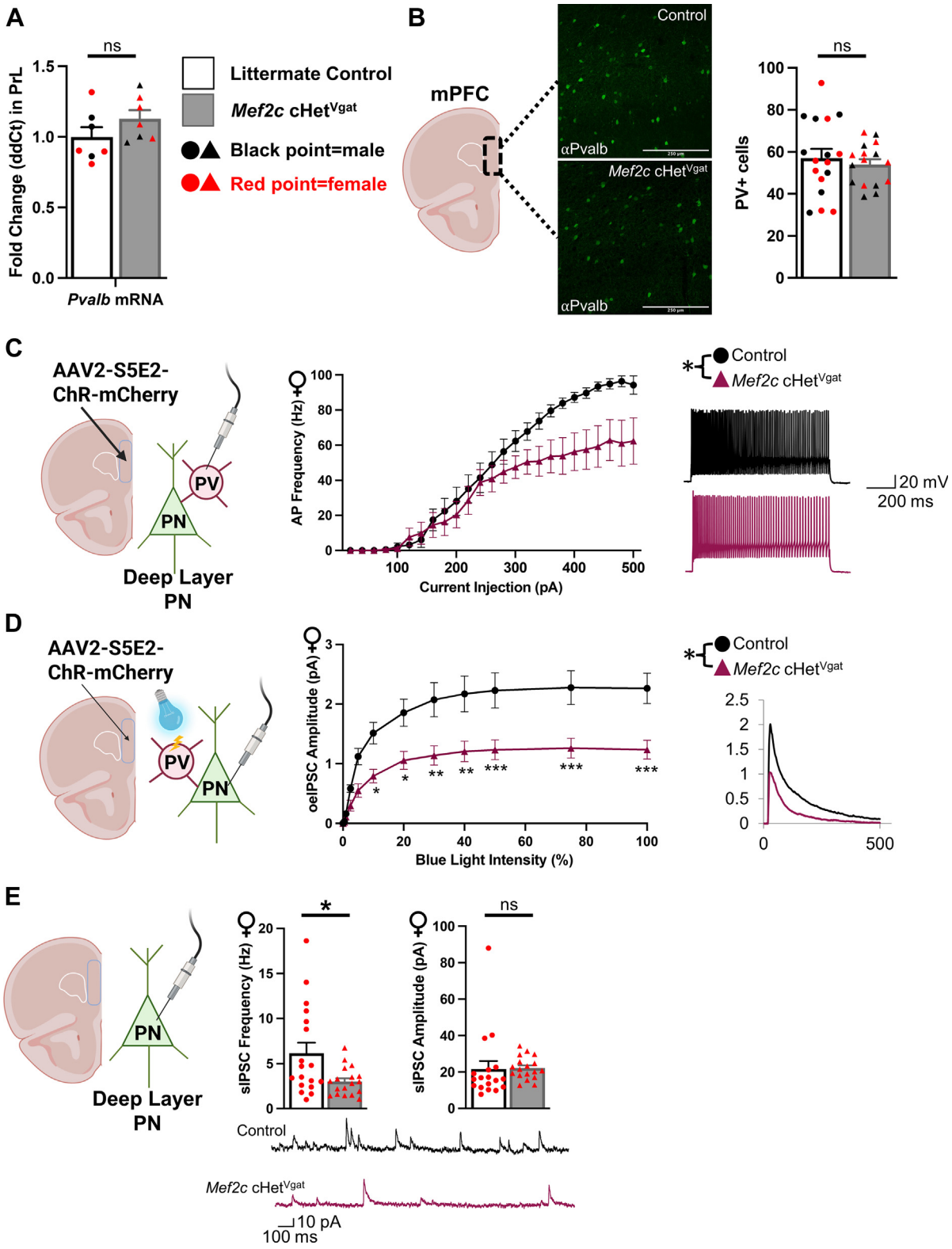

Figure 5. mPFC PV neurons display reduced intrinsic excitability and hypofunction, and PNs receive reduced GABAergic input. **(A)** PV messenger RNA levels are not different between *Mef2c* cHet^{Vgat} (n = 7; 3 male, 4 female) and control (n = 6; 3 male, 4 female) mice in the PFC by quantitative polymerase chain reaction at age 8 weeks. **(B)** The number of PV-expressing cells in the PFC are not different between *Mef2c* cHet^{Vgat} (n = 16; 8 male, 8 female) and control (n =

connectivity of the mPFC during mentalization (63,64). We strongly suspect that PV cell dysfunction is not limited to the mPFC.

Mef2c expression in GABAergic striatal projection neurons is reportedly transient during development and impacts corticostriatal synaptogenesis and ultrasonic vocalizations (65). However, *Mef2c* heterozygosity in VGAT-positive cells in our study did not disrupt USVs during early postnatal periods (Figure S1C in Supplement 1), suggesting that 1 allele of *Mef2c* is sufficient for corticostriatal connectivity and USVs. One interesting observation in *Mef2c* cHet^{Vgat} mice is the reduction in spontaneous alternations in the Y-maze assay, which is often interpreted as a deficit in spatial working memory (66). Notably, PV neurons in the PFC are required for spatial working memory (67), and transient decreases in PV neuron activity in the PFC can irrevocably affect cognitive behavior and gamma oscillations (68). Similar to sociability and working memory, there is evidence for dichotomous regulation of the excitatory and inhibitory tone in the PFC to differentially influence avoidance and approach on the EPM (69).

In this study, we found that *Mef2c* heterozygosity in embryonic SST- or VIP-positive cells did not reproduce phenotypes observed in *Mef2c* cHet^{Vgat} mice, suggesting that MEF2C hypofunction in either of these populations alone does not account for *Mef2c* cHet^{Vgat} behavior phenotypes. Despite robust changes in gene expression, excitability, and inhibitory transmission in PV cells of *Mef2c* cHet^{Vgat} females, *Mef2c* cHet^{Pv} mice did not display deficits in social interaction, EPM, or Y-maze tests, suggesting that reduced MEF2C function in PV cells, at least after the first postnatal week, is dispensable for the assessed behaviors that we examined. Notably, our snRNA-seq data revealed numerous changes in all 4 inhibitory cell clusters in the mPFC of *Mef2c* cHet^{Vgat} females, with the largest changes occurring in the PV^{+} and Lamp5^{+} inhibitory neuron clusters. While Lamp5^{+} cells represented a considerably lower percentage of inhibitory cells than Pvalb^{+} cells in the PFC, LAMP5, a brain-specific membrane protein, has been found to influence evoked GABAergic transmission, and LAMP5-deficient mice had reduced anxiety and deficits in olfactory discrimination (70). Therefore, it seems likely that the phenotypes detected in the *Mef2c* cHet^{Vgat} females are due to the combined effects of multiple GABAergic cell types and/or cell nonautonomous changes in non-GABAergic cells, many of which are impacted at the level of gene expression.

How sex interacts with MEF2C hypofunction in GABAergic cells remains unclear. Current clinical evidence does not suggest a sex bias in ASD symptom prevalence in MCHS (71,72), and both male and female global *Mef2c*$^{+/-}$ mice showed social preference deficits (16). Our previous investigations into *Mef2c* mutant mice (Table 1) have not yielded female-specific phenotypes. We observed possible sex differences between control male and control female mice in 1) prefrontocortical EEG, especially during social interaction periods and not during noninteraction, and 2) in PV neuron excitability, specifically in the 340 to 500 pA current range. These findings suggest sex differences in PFC processing at baseline, and the caveat remains that we are observing a complex interplay between existing sexual dimorphisms and further modification due to MEF2C haploinsufficiency, possibly through regulatory gene expression changes. There are documented sex differences in EEG power in autism; however, the literature on frequency-specific changes in specific contexts is not well-described (73). Because PV neurons play a critical role in generating and maintaining gamma oscillations, the differences that we observed between male and female mice could be attributable to how female cortical fast-spiking neurons are activated by touch, regulated by estrus state, and influenced by estradiol (74). It is possible that estrus-related tuning of interneuron activity and concomitant changes in GABAergic receptor expression (75) may contribute to interneuron cycling, characterized by changes in cortical inhibitory tone. Emerging evidence suggests that excitation/inhibition balance is dynamic and that estrogen can increase PV neuron excitability in the deep layers of the cortex through its actions on estrogen receptor beta, and estrus state can affect inhibition and reduce evoked inhibitory latency (74). These female-specific modifiers could be at play when evaluating PV intrinsic excitability. We conducted a gene-set enrichment analysis in DEGs of PV cells to detect changes in estrogen pathway and signaling; however, we did not observe any significant enrichments. How sex hormones interact with MEF2C's developmental influences on GABAergic neurons will be an important question for future studies.

Neuropsychiatric disorders and neurotypical cognitive function are heavily influenced by excitation/inhibition balance within the brain (43,44). Our findings here suggest that mPFC PV interneurons in *Mef2c* cHet^{Vgat} females are less excitable and show a reduction in inhibitory synaptic transmission onto deep-layer pyramidal neurons. We failed to detect a clear change in PV presynaptic function (by oeIPSC PPR), suggesting that the inhibitory transmission deficit could be due to postsynaptic strength or fewer PV synapses onto deep-layer pyramidal neurons. Analysis of sIPSCs, which involves measurement of all GABAergic synapses rather than isolated PV

17; 8 male, 9 female) mice by immunohistochemistry at age 8 weeks. Representative images of PV immunostaining in the PFC are shown (scale bar = 250 μM). **(C)** AAV2-S5E2-ChR-mCherry was injected into the PFC at age 5 weeks, and whole-cell patch-clamp recordings took place at age 8 weeks. PFC PV neurons from female *Mef2c* cHet^{Vgat} mice (n = 4, 8 cells) elicited fewer action potentials with current injection than female control mice (n = 4, 9 cells). **(D)** When recording from pyramidal neurons after shining blue light atop the PFC to stimulate PV neurons, we observed a decrease in oeIPSC amplitude in female *Mef2c* cHet^{Vgat} (n = 4, 14 cells) compared with female control (n = 4, 16 cells) mice. **(E)** We detected a decrease in sIPSC frequency onto pyramidal neurons, but not amplitude, in the PFC of *Mef2c* cHet^{Vgat} mice (n = 6, 18 cells) compared with control mice (n = 6, 18 cells). Red data points represent females, circles represent control animals, and triangles represent *Mef2c* cHet^{Vgat} mice. Data are reported as mean ± SEM. Statistical significance was determined by unpaired t test for **(A, B)**. Statistical significance was determined by Kolmogorov-Smirnov test for **(C)** and analysis of variance for **(D, E)** (2-way). ns = not significant ($p > .05$), *$p < .05$, **$p < .01$, ***$p < .005$. Outliers were removed using the Grubbs' test. Control mice as a group include Cre-positive mice. cHet, conditional heterozygous; GABA, gamma-aminobutyric acid; mPFC, medial prefrontal cortex; oeIPSC, optogenetically evoked inhibitory postsynaptic current; PN, pyramidal neuron; PV, parvalbumin; sIPSC, spontaneous inhibitory postsynaptic current.

Table 1. Behavioral Phenotypes in *Mef2c* Mutant Mice

Mef2c Mutant	Cre Driver	Locomotor Activity (Jump Count; Distance Traveled)	Y-Maze (% Correct Spontaneous Alternations)	Elevated Plus Maze (Time in Open Arms)	Social Preference	Fear Conditioning (Training, Context, Cue)
Mef2c$^{+/-}$	Prm-cre	↑♂;↑♂	=	↑	↓	=
Mef2c cHet^{Emx1}	Emx1-cre	↑♂;↑♂	NA	↑	=	NA
Mef2c cHet^{Cx3cr1}	Cx3cr1-cre	↑♂;=	NA	=	↓	NA
Mef2c cHet^{Vgat}	Vgat-cre	=;=	↓	↑♀	↓♀	=
Mef2c cHet^{Pcp2}	Pcp2-cre	=	NA	=	=	NA
Mef2c cHet^{Pv}	Pv-cre	=	NA	=	=	NA
Mef2c cHet^{Sst}	Sst-cre	=	=	=	=	=
Mef2c cHet^{Vip}	Vip-cre	↑♂;=	=	=	=	=

↑ indicates an increase compared with control mice; ↓ indicates a decrease compared with control mice; and = indicates no change compared with control mice.
cHet, conditional heterozygous; NA, not assessed.

cells, showed normal sIPSC amplitude, suggesting preserved postsynaptic strength, but we detected a reduction in sIPSC frequency. However, there was no detectable change in IPSC PPR, suggesting that the reduction in frequency is not due to reduced presynaptic function. As such, the findings demonstrate a possible reduction in PV synapses onto deep-layer mPFC pyramidal cells, which will be important to examine in the future.

Conclusions

In this study, we assessed the role of MEF2C hypofunction in developing GABAergic cells using genetic dissection strategies and found that reduced MEF2C function in GABAergic cells produced female-specific deficits in social preference and approach-avoidance behavior. Moreover, our findings revealed significant impacts on mPFC gene expression, basal and social-induced frontocortical EEGs, and PV cell excitability and inhibitory synaptic transmission. Our findings demonstrate an important female-specific role for MEF2C in GABAergic populations for multiple behaviors with relevance to MCHS, including sociability, and provide new mechanistic insights into the essential dosage-sensitive roles for MEF2C in neurotypical development and brain circuit function.

ACKNOWLEDGMENTS AND DISCLOSURES

This work was supported by National Institutes of Health (Grant Nos. TL1 TR001451 and UL1 TR001450 [to JYC], R01 MH111464 [to CWC], K18DC018517 [to HL]), and Simons Foundation Autism Research Initiative Pilot Award (Award No. 649452 [to CWC and HL]).

JYC performed surgeries and collected EEG data. JAR and HL analyzed EEG data and wrote results. JYC performed snRNA-seq tissue collection and nuclei dissociation. SB performed snRNA-seq bioinformatics analyses. JYC and DSP performed molecular/biochemical experiments and data analysis. JYC and AA performed electrophysiology surgeries. ET performed electrophysiology and analyzed electrophysiology data. JYC, AA, and CWC designed experiments, interpreted results, and wrote the paper.

We thank Tom Jhou and Takashi Sato for assistance with EEG recordings, Nathan Phan, Ben Zirlin, and Makoto Taniguchi for technical assistance, the Medical University of South Carolina Translational Science Lab for assistance with snRNA-seq, the Medical University of South Carolina Proteogenomics Facility (NIH GM103499) for access to technical assistance with quantitative polymerase chain reaction, and the COBRE in NeuroDevelopment and Its Disorders (CNDD) Genomics and Bioinformatics Core (P20 GM148302) for bioinformatics analysis.

The authors report no biomedical financial interests or potential conflicts of interest.

ARTICLE INFORMATION

From the Department of Neuroscience, Medical University of South Carolina, Charleston, South Carolina (JYC, ET, DSP, SB, AA, CWC); Medical Scientist Training Program, Medical University of South Carolina, Charleston, South Carolina (JYC); and Department of Pathology and Laboratory Medicine, Medical University of South Carolina, Charleston, South Carolina (JAR, HL).

AA is currently affiliated with Institut du Cerveau-Brain Institute, Paris, France.

Address correspondence to Ahlem Assali, Ph.D., at ahlem_assali@yahoo.fr, or Christopher W. Cowan, Ph.D., at cowanc@musc.edu.

Received Jul 13, 2023; revised Dec 20, 2023; accepted Dec 28, 2023.

Supplementary material cited in this article is available online at https://doi.org/10.1016/j.bpsgos.2024.100289.

REFERENCES

1. Leifer D, Krainc D, Yu YT, McDermott J, Breitbart RE, Heng J, *et al.* (1993): MEF2C, a MADS/MEF2-family transcription factor expressed in a laminar distribution in cerebral cortex. Proc Natl Acad Sci USA 90:1546–1550.
2. Leifer D, Golden J, Kowall NW (1994): Myocyte-specific enhancer binding factor 2C expression in human brain development. Neuroscience 63:1067–1079.
3. Lyons GE, Micales BK, Schwarz J, Martin JF, Olson EN (1995): Expression of mef2 genes in the mouse central nervous system suggests a role in neuronal maturation. J Neurosci 15:5727–5738.
4. Lyons MR, Schwarz CM, West AE (2012): Members of the myocyte enhancer factor 2 transcription factor family differentially regulate Bdnf transcription in response to neuronal depolarization. J Neurosci 32:12780–12785.
5. Lin X, Shah S, Bulleit RF (1996): The expression of MEF2 genes is implicated in CNS neuronal differentiation. Brain Res Mol Brain Res 42:307–316.
6. Zhang Y, Chen K, Sloan SA, Bennett ML, Scholze AR, O'Keeffe S, *et al.* (2014): An RNA-sequencing transcriptome and splicing database of glia, neurons, and vascular cells of the cerebral cortex. J Neurosci 34:11929–11947.
7. Harrington AJ, Raissi A, Rajkovich K, Berto S, Kumar J, Molinaro G, *et al.* (2016): MEF2C regulates cortical inhibitory and excitatory synapses and behaviors relevant to neurodevelopmental disorders. eLife 5:e20059.
8. Mayer C, Hafemeister C, Bandler RC, Machold R, Batista Brito R, Jaglin X, *et al.* (2018): Developmental diversification of cortical inhibitory interneurons. Nature 555:457–462.
9. Deczkowska A, Matcovitch-Natan O, Tsitsou-Kampeli A, Ben-Hamo S, Dvir-Szternfeld R, Spinrad A, *et al.* (2017): Mef2C restrains microglial inflammatory response and is lost in brain ageing in an IFN-I-dependent manner. Nat Commun 8:717.
10. Pulipparacharuvil S, Renthal W, Hale CF, Taniguchi M, Xiao G, Kumar A, *et al.* (2008): Cocaine regulates MEF2 to control synaptic and behavioral plasticity. Neuron 59:621–633.
11. Kamath SP, Chen AI (2019): Myocyte enhancer factor 2c regulates dendritic complexity and connectivity of cerebellar Purkinje cells. Mol Neurobiol 56:4102–4119.
12. Potthoff MJ, Olson EN (2007): MEF2: A central regulator of diverse developmental programs. Development 134:4131–4140.
13. Shalizi AK, Bonni A (2005): brawn for brains: The role of MEF2 proteins in the developing nervous system. Curr Top Dev Biol 69:239–266.
14. Tu S, Akhtar MW, Escorihuela RM, Amador-Arjona A, Swarup V, Parker J, *et al.* (2017): NitroSynapsin therapy for a mouse MEF2C haploinsufficiency model of human autism. Nat Commun 8:1488.
15. Assali A, Harrington AJ, Cowan CW (2019): Emerging roles for MEF2 in brain development and mental disorders. Curr Opin Neurobiol 59:49–58.
16. Harrington AJ, Bridges CM, Berto S, Blankenship K, Cho JY, Assali A, *et al.* (2020): MEF2C hypofunction in neuronal and neuroimmune populations produces MEF2C haploinsufficiency syndrome-like behaviors in mice. Biol Psychiatry 88:488–499.
17. Sundararajan T, Manzardo AM, Butler MG (2018): Functional analysis of schizophrenia genes using GeneAnalytics program and integrated databases. Gene 641:25–34.
18. Lambert JC, Ibrahim-Verbaas CA, Harold D, Naj AC, Sims R, Bellenguez C, *et al.* (2013): Meta-analysis of 74,046 individuals identifies 11 new susceptibility loci for Alzheimer's disease. Nat Genet 45:1452–1458.
19. Hyde CL, Nagle MW, Tian C, Chen X, Paciga SA, Wendland JR, *et al.* (2016): Identification of 15 genetic loci associated with risk of major depression in individuals of European descent. Nat Genet 48:1031–1036.
20. Shadrin AA, Smeland OB, Zayats T, Schork AJ, Frei O, Bettella F, *et al.* (2018): Novel loci associated with attention-deficit/hyperactivity disorder are revealed by leveraging polygenic overlap with educational attainment. J Am Acad Child Adolesc Psychiatry 57:86–95.
21. Rosenthal SL, Kamboh MI (2014): Late-onset Alzheimer's disease genes and the potentially implicated pathways. Curr Genet Med Rep 2:85–101.
22. Mitchell AC, Javidfar B, Pothula V, Ibi D, Shen EY, Peter CJ, *et al.* (2018): MEF2C transcription factor is associated with the genetic and epigenetic risk architecture of schizophrenia and improves cognition in mice. Mol Psychiatry 23:123–132.
23. Le Meur N, Holder-Espinasse M, Jaillard S, Goldenberg A, Joriot S, Amati-Bonneau P, *et al.* (2010): MEF2C haploinsufficiency caused by either microdeletion of the 5q14.3 region or mutation is responsible for severe mental retardation with stereotypic movements, epilepsy and/or cerebral malformations. J Med Genet 47:22–29.
24. Zweier M, Gregor A, Zweier C, Engels H, Sticht H, Wohlleber E, *et al.* (2010): Mutations in MEF2C from the 5q14.3q15 microdeletion syndrome region are a frequent cause of severe mental retardation and diminish MECP2 and CDKL5 expression. Hum Mutat 31:722–733.
25. Vrečar I, Innes J, Jones EA, Kingston H, Reardon W, Kerr B, *et al.* (2017): Further clinical delineation of the MEF2C haploinsufficiency syndrome: Report on new cases and literature review of severe neurodevelopmental disorders presenting with seizures, absent speech, and involuntary movements. J Pediatr Genet 6:129–141.
26. Paciorkowski AR, Traylor RN, Rosenfeld JA, Hoover JM, Harris CJ, Winter S, *et al.* (2013): MEF2C haploinsufficiency features consistent hyperkinesis, variable epilepsy, and has a role in dorsal and ventral neuronal developmental pathways. Neurogenetics 14:99–111.
27. Zweier M, Rauch A (2011): The MEF2C-related and 5q14.3q15 microdeletion syndrome. Mol Syndromol 2:164–170.
28. Mikhail FM, Lose EJ, Robin NH, Descartes MD, Rutledge KD, Rutledge SL, *et al.* (2011): Clinically relevant single gene or intragenic deletions encompassing critical neurodevelopmental genes in patients with developmental delay, mental retardation, and/or autism spectrum disorders. Am J Med Genet A 155A:2386–2396.
29. Novara F, Beri S, Giorda R, Ortibus E, Nageshappa S, Darra F, *et al.* (2010): Refining the phenotype associated with MEF2C haploinsufficiency. Clin Genet 78:471–477.
30. Engels H, Wohlleber E, Zink A, Hoyer J, Ludwig KU, Brockschmidt FF, *et al.* (2009): A novel microdeletion syndrome involving 5q14.3-q15: Clinical and molecular cytogenetic characterization of three patients. Eur J Hum Genet 17:1592–1599.
31. Berland S, Houge G (2010): Late-onset gain of skills and peculiar jugular pit in an 11-year-old girl with 5q14.3 microdeletion including MEF2C. Clin Dysmorphol 19:222–224.
32. Bienvenu T, Diebold B, Chelly J, Isidor B (2013): Refining the phenotype associated with MEF2C point mutations. Neurogenetics 14:71–75.
33. Tonk V, Kyhm JH, Gibson CE, Wilson GN (2011): Interstitial deletion 5q14. 3q21.3 with MEF2C haploinsufficiency and mild phenotype: When more is less. Am J Med Genet A 155A:1437–1441.
34. Nowakowska BA, Obersztyn E, Szymańska K, Bekiesińska-Figatowska M, Xia Z, Ricks CB, *et al.* (2010): Severe mental retardation, seizures, and hypotonia due to deletions of MEF2C. Am J Med Genet B Neuropsychiatr Genet 153B:1042–1051.
35. Gosselin D, Skola D, Coufal NG, Holtman IR, Schlachetzki JCM, Sajti E, *et al.* (2017): An environment-dependent transcriptional network specifies human microglia identity. Science 356:eaal3222.
36. Tamamaki N, Yanagawa Y, Tomioka R, Miyazaki J, Obata K, Kaneko T (2003): Green fluorescent protein expression and colocalization with calretinin, parvalbumin, and somatostatin in the GAD67-GFP knock-in mouse. J Comp Neurol 467:60–79.
37. Hendry SH, Schwark HD, Jones EG, Yan J (1987): Numbers and proportions of GABA-immunoreactive neurons in different areas of monkey cerebral cortex. J Neurosci 7:1503–1519.
38. Ren JQ, Aika Y, Heizmann CW, Kosaka T (1992): Quantitative analysis of neurons and glial cells in the rat somatosensory cortex, with special reference to GABAergic neurons and parvalbumin-containing neurons. Exp Brain Res 92:1–14.
39. Sahara S, Yanagawa Y, O'Leary DD, Stevens CF (2012): The fraction of cortical GABAergic neurons is constant from near the start of cortical neurogenesis to adulthood. J Neurosci 32:4755–4761.

40. Markram H, Toledo-Rodriguez M, Wang Y, Gupta A, Silberberg G, Wu C (2004): Interneurons of the neocortical inhibitory system. Nat Rev Neurosci 5:793–807.
41. Hattori R, Kuchibhotla KV, Froemke RC, Komiyama T (2017): Functions and dysfunctions of neocortical inhibitory neuron subtypes. Nat Neurosci 20:1199–1208.
42. Batista-Brito R, Fishell G (2009): The developmental integration of cortical interneurons into a functional network. Curr Top Dev Biol 87:81–118.
43. Sohal VS, Rubenstein JLR (2019): Excitation-inhibition balance as a framework for investigating mechanisms in neuropsychiatric disorders. Mol Psychiatry 24:1248–1257.
44. Ferguson BR, Gao WJ (2018): PV interneurons: Critical regulators of E/I balance for prefrontal cortex-dependent behavior and psychiatric disorders. Front Neural Circuits 12:37.
45. Isaacson JS, Scanziani M (2011): How inhibition shapes cortical activity. Neuron 72:231–243.
46. Lunden JW, Durens M, Phillips AW, Nestor MW (2019): Cortical interneuron function in autism spectrum condition. Pediatr Res 85:146–154.
47. Marín O (2012): Interneuron dysfunction in psychiatric disorders. Nat Rev Neurosci 13:107–120.
48. Vong L, Ye C, Yang Z, Choi B, Chua S, Lowell BB (2011): Leptin action on GABAergic neurons prevents obesity and reduces inhibitory tone to POMC neurons. Neuron 71:142–154.
49. Lin Q, Schwarz J, Bucana C, Olson EN (1997): Control of mouse cardiac morphogenesis and myogenesis by transcription factor MEF2C. Science 276:1404–1407.
50. Assali A, Chenaux G, Cowan CW (2022): EphB1 controls proper long-range cortical axon guidance through a cell non-autonomous role in GABAergic cells. bioRxiv. https://doi.org/10.1101/2022.02.28.482352.
51. Taniguchi H, He M, Wu P, Kim S, Paik R, Sugino K, *et al.* (2011): A resource of Cre driver lines for genetic targeting of GABAergic neurons in cerebral cortex. Neuron 71:995–1013.
52. Urban KR, Layfield DM, Griffin AL (2014): Transient inactivation of the medial prefrontal cortex impairs performance on a working memory-dependent conditional discrimination task. Behav Neurosci 128:639–643.
53. Ferguson BR, Gao WJ (2018): Thalamic control of cognition and social behavior via regulation of gamma-aminobutyric acidergic signaling and excitation/inhibition balance in the medial prefrontal cortex. Biol Psychiatry 83:657–669.
54. Shah AA, Treit D (2003): Excitotoxic lesions of the medial prefrontal cortex attenuate fear responses in the elevated-plus maze, social interaction and shock probe burying tests. Brain Res 969:183–194.
55. Telese F, Ma Q, Perez PM, Notani D, Oh S, Li W, *et al.* (2015): LRP8-reelin-regulated neuronal enhancer signature underlying learning and memory formation. Neuron 86:696–710.
56. Shangguan Y, Xu X, Ganbat B, Li Y, Wang W, Yang Y, *et al.* (2018): CNTNAP4 impacts epilepsy through GABAA receptors regulation: Evidence from temporal lobe epilepsy patients and mouse models. Cereb Cortex 28:3491–3504.
57. Karayannis T, Au E, Patel JC, Kruglikov I, Markx S, Delorme R, *et al.* (2014): Cntnap4 differentially contributes to GABAergic and dopaminergic synaptic transmission. Nature 511:236–240.
58. Bicks LK, Yamamuro K, Flanigan ME, Kim JM, Kato D, Lucas EK, *et al.* (2020): Prefrontal parvalbumin interneurons require juvenile social experience to establish adult social behavior. Nat Commun 11:1003.
59. Yamamuro K, Bicks LK, Leventhal MB, Kato D, Im S, Flanigan ME, *et al.* (2020): A prefrontal–paraventricular thalamus circuit requires juvenile social experience to regulate adult sociability in mice. Nat Neurosci 23:1240–1252.
60. Bicks LK, Koike H, Akbarian S, Morishita H (2015): Prefrontal cortex and social cognition in mouse and man. Front Psychol 6:1805.
61. Barak B, Feng G (2016): Neurobiology of social behavior abnormalities in autism and Williams syndrome. Nat Neurosci 19:647–655.
62. Franklin TB, Silva BA, Perova Z, Marrone L, Masferrer ME, Zhan Y, *et al.* (2017): Prefrontal cortical control of a brainstem social behavior circuit. Nat Neurosci 20:260–270.
63. Murdaugh DL, Shinkareva SV, Deshpande HR, Wang J, Pennick MR, Kana RK (2012): Differential deactivation during mentalizing and classification of autism based on default mode network connectivity. PLoS One 7:e50064.
64. Bateman A, Fonagy P (2010): Mentalization based treatment for borderline personality disorder. World Psychiatry 9:11–15.
65. Chen YC, Kuo HY, Bornschein U, Takahashi H, Chen SY, Lu KM, *et al.* (2016): Foxp2 controls synaptic wiring of corticostriatal circuits and vocal communication by opposing Mef2c. Nat Neurosci 19:1513–1522.
66. Kraeuter AK, Guest PC, Sarnyai Z (2019): The Y-maze for assessment of spatial working and reference memory in mice. Methods Mol Biol 1916:105–111.
67. Murray AJ, Woloszynowska-Fraser MU, Ansel-Bollepalli L, Cole KL, Foggetti A, Crouch B, *et al.* (2015): Parvalbumin-positive interneurons of the prefrontal cortex support working memory and cognitive flexibility. Sci Rep 5:16778.
68. Canetta SE, Holt ES, Benoit LJ, Teboul E, Sahyoun GM, Ogden RT, *et al.* (2022): Mature parvalbumin interneuron function in prefrontal cortex requires activity during a postnatal sensitive period. eLife 11:e80324.
69. Sánchez-Bellot C, AlSubaie R, Mishchanchuk K, Wee RWS, MacAskill AF (2022): Two opposing hippocampus to prefrontal cortex pathways for the control of approach and avoidance behaviour. Nat Commun 13:339.
70. Tiveron MC, Beurrier C, Céni C, Andriambao N, Combes A, Koehl M, *et al.* (2016): LAMP5 fine-tunes GABAergic synaptic transmission in defined circuits of the mouse brain. PLOS ONE 11:e0157052.
71. Cooley Coleman JA, Sarasua SM, Moore HW, Boccuto L, Cowan CW, Skinner SA, DeLuca JM (2022): Clinical findings from the landmark MEF2C-related disorders natural history study. Mol Genet Genomic Med 10:e1919.
72. Raviglione F, Douzgou S, Scala M, Mingarelli A, D'Arrigo S, Freri E, *et al.* (2021): Electroclinical features of MEF2C haploinsufficiency-related epilepsy: A multicenter European study. Seizure 88:60–72.
73. Williams OOF, Coppolino M, Perreault ML (2021): Sex differences in neuronal systems function and behaviour: Beyond a single diagnosis in autism spectrum disorders. Transl Psychiatry 11:625.
74. Clemens AM, Lenschow C, Beed P, Li L, Sammons R, Naumann RK, *et al.* (2019): Estrus-cycle regulation of cortical inhibition. Curr Biol 29:605–615.e6.
75. Maguire JL, Stell BM, Rafizadeh M, Mody I (2005): Ovarian cycle–linked changes in GABA(A) receptors mediating tonic inhibition alter seizure susceptibility and anxiety. Nat Neurosci 8:797–804.